

# Self-Supervised Learning of Linear Precoders under Non-Linear PA Distortion for Energy-Efficient Massive MIMO Systems

Thomas Feys\*, Xavier Mestre<sup>†</sup>, François Rottenberg\*

\*KU Leuven, ESAT-WaveCore, Dramco, 9000 Ghent, Belgium

<sup>†</sup>ISPIC, Centre Tecnologic Telecomunicacions Catalunya, Barcelona, Spain.

**Abstract**—Massive multiple input multiple output (MIMO) systems are typically designed under the assumption of linear power amplifiers (PAs). However, PAs are typically most energy-efficient when operating close to their saturation point, where they cause non-linear distortion. Moreover, when using conventional precoders, this distortion coherently combines at the user locations, limiting performance. As such, when designing an energy-efficient massive MIMO system, this distortion has to be managed. In this work, we propose the use of a neural network (NN) to learn the mapping between the channel matrix and the precoding matrix, which maximizes the sum rate in the presence of this non-linear distortion. This is done for a third-order polynomial PA model for both the single and multi-user case. By learning this mapping a significant increase in energy efficiency is achieved as compared to conventional precoders and even as compared to perfect digital pre-distortion (DPD), in the saturation regime.

**Index Terms**—Self-supervised learning, massive MIMO, linear precoding, non-linear power amplifier, neural networks.

## I. INTRODUCTION

### A. Problem Formulation

The estimated carbon footprint and electricity usage of the wireless communications sector continues to rise [1]. As such, in the race to reduce carbon emissions and energy consumption by 2030 as stated by Europe’s Green Deal [2] and the United Nations Sustainable Development Goals (SDGs) [3], the wireless communications sector is falling behind. In wireless communication systems, the PA accounts for a large part of the energy consumption of a base station (BS) [4]. As such, it is vital to operate it in an energy-efficient manner. However, PAs are most efficient close to their saturation point, where non-linear distortion arises. This leads to a trade-off between energy efficiency and linearity. In the past, linearity has taken the upper hand in this trade-off given that non-linear distortion limits the system capacity. As such, the PA is typically operated at a certain back-off power in order to stay in the linear regime, which is detrimental for its energy efficiency. For the current technology, the energy efficiency of the PA is typically as low as 5 – 30% [4], [5]. In this work, we study how to operate the PAs of a massive MIMO system closer to saturation by learning a precoding matrix that boosts

performance in the presence of non-linear distortion. By doing so, the same capacity can be achieved while using less back-off, which improves the energy efficiency.

### B. State-of-the-Art

As stated in the previous section, a large back-off is typically required to stay in the linear regime of the PA which limits its energy efficiency. However, given the need to reduce energy consumption, this solution is no longer viable. Efforts to linearize the PA such as DPD are used in practical systems [6]. However, DPD techniques have a significant complexity burden, especially in massive MIMO where they have to be deployed at each antenna. Moreover, their performance is limited by clipping, i.e., the PA can only be linearized up to the saturation point, so that a relatively large back-off is still required. More recent solutions incorporate knowledge of the distortion into the precoder design [7]–[10]. This allows for the spatial suppression of the distortion in the user directions, producing considerable gains over classical precoders. Unfortunately, these solutions are still limited in their practical implementation. In [10] the solution to the precoding problem is obtained by solving a non-convex optimization problem with a projected gradient descent-based procedure. Given that the problem is non-convex, the procedure is executed multiple times in order to obtain a close-to-optimal solution. As an alternative solution for the problem, the authors in [7] derived a, globally optimal, closed-form solution for the simplified single-user case and a line-of-sight (LOS) channel, which was later extended to a general channel in [8]. There is thus a need for a solution that has low complexity and can address the challenging case of spatial user multiplexing.

### C. Contributions

In this work, we propose the use of a NN to find a mapping from the channel matrix to the precoding matrix. This mapping is learned under the presence of a non-linear PA operated close to its saturation point, which introduces non-linear distortion. The need for machine learning arises from the non-linear and non-convex nature of the problem, which limits classical linear signal processing solutions. By learning the non-linear mapping from channel matrix to precoding matrix, a lot of the complexity is offloaded to the training step, which reduces the online computational complexity. This allows for a practical

This work was made possible by a mobility grant provided by the (Fonds wetenschappelijk Onderzoek) FWO with filenumber V424222N and a short-term scientific mission grant by the COST ACTION CA20120 INTERACT.

solution to the precoding problem under the presence of non-linear PA distortion even in the multi-user case, which has not been addressed in previous works. As such, this opens perspectives to operate PAs closer to their saturation point, which drastically increases their energy efficiency.

**Notations:** Vectors and matrices are denoted by bold lowercase and bold uppercase letters respectively. Superscripts  $(\cdot)^*$ ,  $(\cdot)^\top$  and  $(\cdot)^H$  stand for the conjugate, transpose and Hermitian transpose operators respectively. Subscripts  $(\cdot)_m$  and  $(\cdot)_k$  denote the antenna and user index. The expectation is denoted by  $\mathbb{E}(\cdot)$ . The  $M \times M$  identity matrix is given by  $\mathbf{I}_M$ . The main diagonal of a square matrix  $\mathbf{A}$  is given by  $\text{diag}(\mathbf{A})$ . The trace of a matrix is given by  $\text{Tr}(\cdot)$ . The element-wise or Hadamard product of two matrices is denoted by  $\mathbf{A} \odot \mathbf{B}$ . The element at location  $(i, j)$  in matrix  $\mathbf{A}$  is indicated as  $[\mathbf{A}]_{i,j}$ .

## II. SYSTEM MODEL

In this work, we consider a massive MIMO system where the BS is equipped with  $M$  transmit antennas and  $K$  single-antenna users are spatially multiplexed. The complex symbol intended for user  $k$  is denoted as  $s_k$  and is assumed to be zero mean circularly symmetric complex Gaussian with unit variance. The symbols between different users are assumed to be uncorrelated. The linearly precoded symbol at antenna  $m$  is denoted by

$$x_m = \sum_{k=0}^{K-1} w_{m,k} s_k, \quad (1)$$

where  $w_{m,k}$  is the precoding coefficient for user  $k$  at antenna  $m$ . In matrix form, the precoded symbol vector  $\mathbf{x} \in \mathbb{C}^{M \times 1}$  is

$$\mathbf{x} = \mathbf{W}\mathbf{s}, \quad (2)$$

where  $\mathbf{W} \in \mathbb{C}^{M \times K}$  is the precoding matrix and  $\mathbf{s} \in \mathbb{C}^{K \times 1}$  the symbol vector. The amplified transmit vector  $\mathbf{y} \in \mathbb{C}^{M \times 1}$  is then given by

$$\mathbf{y} = \phi(\mathbf{x}), \quad (3)$$

where  $\phi(\cdot)$  denotes the element-wise non-linear transformation caused by the PAs. The received signal vector  $\mathbf{r} \in \mathbb{C}^{K \times 1}$  is

$$\mathbf{r} = \mathbf{H}^\top \mathbf{y} + \mathbf{v} = \mathbf{H}^\top \phi(\mathbf{W}\mathbf{s}) + \mathbf{v},$$

with  $\mathbf{H} \in \mathbb{C}^{M \times K}$  being the channel matrix. Each of its elements is assumed to be an independently and identically distributed (i.i.d.) Rayleigh channel with zero mean and unit variance. The vector  $\mathbf{v} \in \mathbb{C}^{K \times 1}$  contains i.i.d. zero mean complex Gaussian noise samples with variance  $\sigma_v^2$ .

### A. Modeling of PA Non-Linearities

In this work, the non-linear PA is modeled as a third-order complex valued polynomial [11]. The output of the PA at antenna  $m$  is given by

$$\phi(x_m) = \beta_1 x_m + \beta_3 x_m |x_m|^2, \quad (4)$$

where  $\beta_1$  and  $\beta_3$  are complex coefficients that model both amplitude modulation to amplitude modulation (AM/AM) and

amplitude modulation to phase modulation (AM/PM) distortion. This third-order model is valid as the PA enters saturation, given that the higher-order polynomial terms have a small contribution in this regime.

### B. Optimization Problem

An achievable sum rate  $R_{\text{sum}}$ , i.e., a lower bound on the capacity, can be obtained by considering that the noise and distortion are jointly Gaussian distributed and independent from the data symbols, which can be seen as a worst case

$$R_{\text{sum}} = \sum_{k=0}^{K-1} \log_2(1 + \text{SNIDR}_k), \quad (5)$$

where  $\text{SNIDR}_k$  is the signal-to-noise-and-interference-and-distortion ratio (SNIDR) at user  $k$ . It can be computed based on the Bussgang decomposition [12], which states that the received signal for user  $k$  can be written as  $r_k = B_k s_k + d_k + v_k$ . Here,  $d_k$  captures both the non-linear distortion and inter-user interference, which is uncorrelated to the transmit signal  $s_k$  and the noise  $v_k$ . The linear gain is given by  $B_k = \mathbb{E}(r_k s_k^*) / p_k$ , with  $p_k = \mathbb{E}(s_k s_k^*)$  [12]. The received signal variance for user  $k$  is given by  $|B_k|^2 p_k$ . The distortion and inter-user interference can be computed as  $\mathbb{E}(|d_k|^2) = \mathbb{E}(|r_k|^2) - |B_k|^2 p_k - \sigma_{v_k}^2$ , given that  $d_k$ ,  $s_k$  and  $v_k$  are uncorrelated. The SNIDR for user  $k$  is then given by

$$\text{SNIDR}_k = \frac{|B_k|^2 p_k}{\mathbb{E}(|d_k|^2) + \sigma_v^2}. \quad (6)$$

This general expression for the SNIDR can be evaluated numerically and is used for the simulations in section IV.

For training the NN, the specific case of a third-order PA model is assumed, which simplifies the expression. By applying Bussgang's theorem [12] to the amplification stage, we can write the amplified signal as

$$\phi(\mathbf{x}) = \mathbf{G}\mathbf{x} + \mathbf{e}, \quad (7)$$

with  $\mathbf{e} \in \mathbb{C}^{M \times 1}$  the non-linear distortion term and  $\mathbf{G} \in \mathbb{C}^{M \times M}$  a diagonal matrix containing the Bussgang gains with the diagonal entries being  $[\mathbf{G}]_{m,m} = \mathbb{E}[\phi(x_m) x_m^*] / \mathbb{E}[|x_m|^2]$ . When assuming the third-order polynomial model given in equation (4) and linear precoding ( $\mathbf{x} = \mathbf{W}\mathbf{s}$ ), we can write the gain matrix  $\mathbf{G}$  as a function of the precoding matrix  $\mathbf{W}$  [10]

$$\mathbf{G}(\mathbf{W}) = \beta_1 \mathbf{I}_M + 2\beta_3 \text{diag}(\mathbf{C}_x). \quad (8)$$

This expression is valid when assuming that all PAs have the same polynomial coefficients. The input covariance matrix is given by  $\mathbf{C}_x = \mathbb{E}[\mathbf{x}\mathbf{x}^H] = \mathbf{W}\mathbf{W}^H$ . From [10], the covariance matrix of the non-linear distortion  $\mathbf{e}$  can be derived as

$$\mathbf{C}_e(\mathbf{W}) = 2|\beta_3|^2 \mathbf{C}_x \odot |\mathbf{C}_x|^2. \quad (9)$$

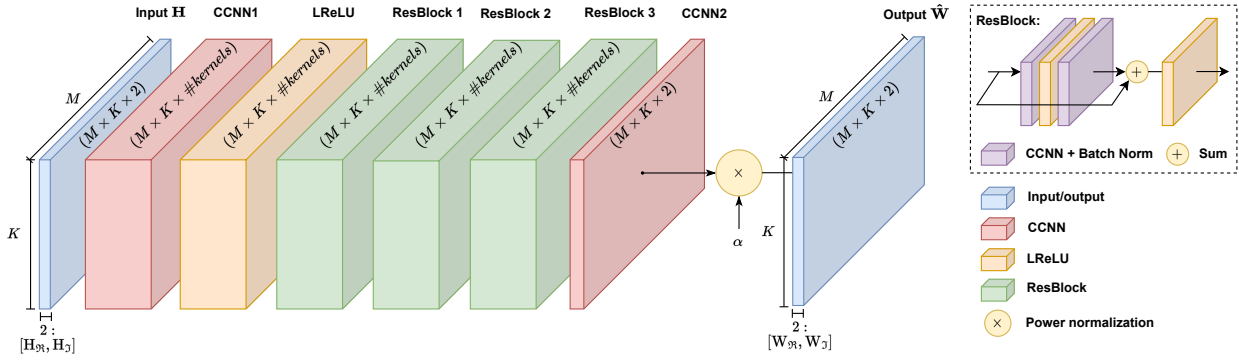


Fig. 1. Circular convolutional neural network architecture.

The received signal at user  $k$  can then be written as

$$r_k = \underbrace{\mathbf{h}_k^T \mathbf{G}(\mathbf{W}) \mathbf{w}_k}_{\text{desired signal}} s_k + \underbrace{\sum_{k' \neq k} \mathbf{h}_k^T \mathbf{G}(\mathbf{W}) \mathbf{w}_{k'}}_{\text{inter-user interference}} s_{k'} \quad (10)$$

$$+ \underbrace{\mathbf{h}_k^T \mathbf{e}}_{\text{received non-linear distortion}} + \underbrace{v_k}_{\text{noise}}. \quad (11)$$

This leads to the following SNIDR expression for user  $k$

$$\text{SNIDR}_k(\mathbf{W}) = \frac{|\mathbf{h}_k^T \mathbf{G}(\mathbf{W}) \mathbf{w}_k|^2}{\sum_{k' \neq k} |\mathbf{h}_k^T \mathbf{G}(\mathbf{W}) \mathbf{w}_{k'}|^2 + \mathbf{h}_k^T \mathbf{C}_e(\mathbf{W}) \mathbf{h}_k + \sigma_v^2}. \quad (12)$$

Given this expression for the SNIDR, an achievable sum rate can be computed using eq. (5). As such, the optimization problem we aim to solve can be formulated as

$$\begin{aligned} \max_{\mathbf{W}} \quad & R_{\text{sum}}(\mathbf{W}) \\ \text{s.t.} \quad & \mathbb{E} \left( \sum_{m=0}^{M-1} |x_m|^2 \right) = \text{Tr}(\mathbf{W}\mathbf{W}^H) \leq P_T, \end{aligned} \quad (13)$$

where  $P_T$  is the total transmit power. The aim is thus to find a precoding matrix which maximizes the sum rate, subject to a power constraint<sup>1</sup>, while the system is affected by PA nonlinearities.

### III. NEURAL NETWORK-BASED PRECODER

Given the optimization problem defined in equation (13), we propose a NN  $f : \mathbb{C}^{M \times K} \mapsto \mathbb{C}^{M \times K}$  which learns a mapping from channel matrix  $\mathbf{H}$  to precoding matrix  $\hat{\mathbf{W}}$ . The NN represents a learned non-linear function

$$\hat{\mathbf{W}} = f(\mathbf{H}; \theta), \quad (14)$$

where  $\theta$  are the learned parameters of the NN.

<sup>1</sup>For simplicity, the power constraint is taken before the PA, which neglects the non-linearly amplified power, which is small compared to the full transmit power.

#### A. Neural Network Architecture

A fully connected neural network can be used to learn the mapping between channel matrix  $\mathbf{H}$  and precoding matrix  $\hat{\mathbf{W}}$ . However, when  $M$  becomes large, the precoding problem becomes high dimensional. Additionally, the architecture of fully connected neural networks is structurally very general due to the high number of tunable parameters, which makes the training of these networks very complex. Hence, it is beneficial to select a neural network architecture which has a structure (i.e., inductive bias) that suits the learning task. The inductive bias of a network constrains the functions which can be learned, reducing the size of the hypothesis space covered by the NN. When the inductive bias matches the learning task, i.e., the desired function can still be well approximated by the selected architecture, the learning performance can be improved while the training complexity is reduced [13].

From [14], we know that the precoding task is permutation equivariant with respect to users and antennas, i.e., if the order of the users in the channel matrix  $\mathbf{H}$  changes, the order of the precoding vectors changes accordingly but the sum rate stays the same. The same analysis is valid when the order of the antennas changes. NNs that fit this property are the graph neural network (GNN) and circular convolutional neural network (CCNN) which were proposed for precoding in [14].

In this work, the CCNN illustrated in Figure 1 is used to learn the precoding task. This network consists of a CCNN layer with leaky rectified linear unit (LReLU) activation, followed by three residual blocks, a final CCNN layer and a power normalization layer to satisfy the power constraint. Each residual block consists of a CCNN layer followed by a batch normalization layer, a LReLU activation and another CCNN layer, after which this output is added to the input of the block and a final LReLU activation is applied. The skip connections used in these residual blocks ensure stable gradients during training [15]. Each CCNN layer, has a kernel size of  $9 \times 3$  and learns 256 kernels, except for the final CCNN layer where only two kernels are learned in order to produce the desired output shape of  $M \times K \times 2$  where the final dimension represents the real and imaginary parts of the precoding matrix. Note that the kernel size of the convolutions is selected to ensure

global receptive field, meaning that each output feature (i.e., element of the precoding matrix) depends on the entire input (i.e., the full channel matrix) [16]. A kernel size of  $9 \times 3$  produces a receptive field of  $65 \times 17$  (computed using the open source library from [16]). The slope coefficient of the LReLU activation for all layers is set to 0.01. The power normalization layer consists of a scalar normalization given by

$$\hat{\mathbf{W}}^{norm} = \alpha \hat{\mathbf{W}}, \quad (15)$$

with  $\alpha = \sqrt{P_T / \text{Tr}(\hat{\mathbf{W}}\hat{\mathbf{W}}^H)}$ .

### B. Training and Hyperparameter Selection

The NN  $f(\mathbf{H}; \boldsymbol{\theta})$  is trained in a self-supervised manner by maximizing the sum rate in order to obtain the NN parameters

$$\boldsymbol{\theta}^* = \arg \min_{\boldsymbol{\theta}} -R_{\text{sum}}(f(\mathbf{H}; \boldsymbol{\theta})). \quad (16)$$

The parameters of the NN are updated using the Adam optimizer [17]. The training set consists of 200000 generated Rayleigh fading channels sampled from a complex normal distribution with zero mean and variance one  $[\mathbf{H}]_{i,j} \sim \mathcal{CN}(0, 1)$ . The hyperparameters are selected by using a validation set of size 2000, while for the simulations performed in section IV, an independent test set of size 10000 is used. For training, a batch size of 256 is used, with an initial learning rate of  $5 \times 10^{-3}$ , which is reduced if the validation loss reaches a plateau. The network is trained for 50 epochs with early stopping if the validation loss does not further decrease.

TABLE I  
PA PARAMETERS AT DIFFERENT BACK-OFF VALUES ( $\beta_1 = 1$ ).

IBO [dB]	-9	-7.5	-6	-4.5	-3	-1.5	0
$\beta_3 (\cdot 10^{-3})$	-19.93	-30.69	-42.26	-56.13	-77.82	-117.3	-159.1
	-10.80j	-18.85j	-24.91j	-30.06j	-40.12j	-65.01j	-79.25j

## IV. SIMULATIONS

For the following simulations, the polynomial coefficients, which are assumed to be equal across all PAs, are obtained by a least squares regression of the third-order model to the modified Rapp model [18]. The modified Rapp model contains both third and higher-order effects. The AM/AM and AM/PM distortion of this model are

$$\phi_{\text{AM-AM}}(x_m) = \frac{|x_m|}{\left(1 + \left|\frac{x_m}{\sqrt{p_{\text{sat}}}}\right|^{2S}\right)^{\frac{1}{2S}}} \quad (17)$$

$$\phi_{\text{AM-PM}}(x_m) = \frac{A|x_m|^q}{1 + \left|\frac{x_m}{B}\right|^q}. \quad (18)$$

The AM/AM and AM/PM distortion are then applied to the signal as follows

$$\phi(x_m) = \phi_{\text{AM-AM}}(x_m)e^{j(\angle x_m + \phi_{\text{AM-PM}}(x_m))}. \quad (19)$$

In order to obtain the polynomial coefficients in Table I, the modified Rapp model coefficients are set as follows<sup>2</sup>:  $S = 2$ ,

<sup>2</sup>Adapted from [19] to a PA with unit gain.

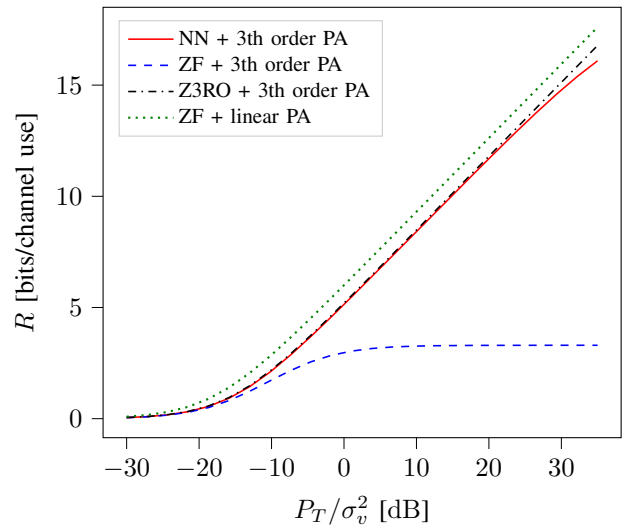


Fig. 2. Achievable rates averaged over 500 channel realizations taken from the test set, for  $M = 64$  and  $K = 1$ . Comparing the NN precoder against ZF (MRT) and the Z3RO precoder from [7].

$q = 4$ ,  $A = -0.315$ ,  $B = 1.137$  and the saturation power of the PA  $p_{\text{sat}}$  is scaled in order to produce the desired input back-off (IBO) according to  $\text{IBO} = p_{\text{in}}/p_{\text{sat}}$ , with  $p_{\text{in}}$  being the average input power at each PA. Additionally, the proposed solution is compared against a perfect DPD. This can be modeled as a linear AM/AM characteristic up to a certain saturation point where the output of the PA is clipped [11]. The AM/AM characteristic is thus modeled as

$$\phi_{\text{AM-AM}}(x_m) = \begin{cases} |x_m| & \text{for } |x_m| \leq \sqrt{p_{\text{sat}}} \\ \sqrt{p_{\text{sat}}} & \text{for } |x_m| > \sqrt{p_{\text{sat}}} \end{cases}, \quad (20)$$

while the AM/PM conversion is zero.

Furthermore, for all simulations, the total transmit power is  $P_T = M$ . Hence, the average power at the input of each PA is  $p_{\text{in}} = P_T/M = 1$ . The linear PA gain is set to one. Training and testing are done at an IBO of  $-3$  dB, unless specified otherwise, this saturates the PAs much more than current cellular systems that require 9-12 dB back-off. The polynomial coefficients corresponding to the IBO value can be found in Table I. During training,  $P_T/\sigma_v^2$  is set to 20 dB. After training, the NNs are evaluated based on the sum rate given in (5).

### A. Single-User Case

In this section, the single-user scenario is considered ( $K = 1$ ), and the ZF precoder becomes the conventional maximum ratio transmission (MRT) precoder as no user interference needs to be canceled. The ZF precoder is designed under the assumption of a linear PA. As a consequence, when a non-linear PA is present, the user performance will be degraded as compared to the linear case. This can be seen in Fig. 2, where the achievable rate of the ZF precoder is depicted as a function of  $P_T/\sigma_v^2$  when considering a linear PA and the non-linear PA model from (4). In the single-user case, the Z3RO precoder

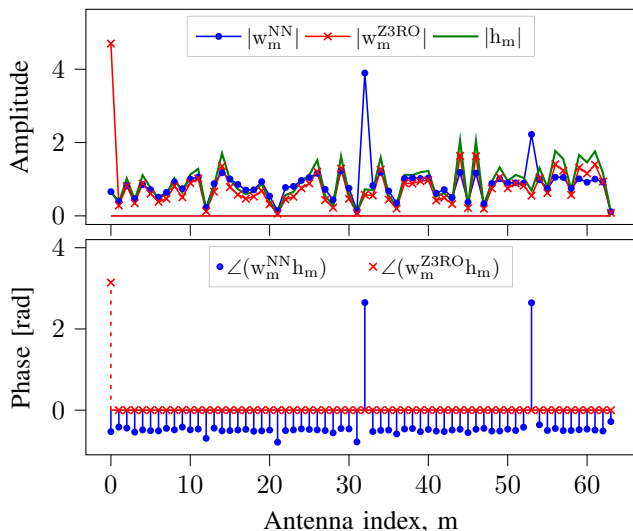


Fig. 3. Modulus of channel and precoding coefficients for the NN and Z3RO (top). Phase of the respective precoding coefficients multiplied with the channel coefficient (bottom). Both precoders saturate one (or a few) antennas with opposite phase shifts, to cancel distortion.

from [7] provides a solution that mitigates the third-order distortion in the user direction, which comes at the cost of a small reduction in array gain. The Z3RO precoder saturates one (or a few) of the antennas with an opposite phase shift. When comparing the NN precoder against the Z3RO precoder in Fig. 2, we see that the NN achieves similar performance as the Z3RO precoder, i.e., the rate is not limited by distortion but grows linearly with  $P_T/\sigma_v^2$ . Indeed, when comparing the amplitude and phase of both precoders in Fig. 3, it is clear that the NN also saturates one or a few of the antennas with an opposite phase shift. In conclusion, for  $K = 1$ , the NN has learned a similar precoding structure as the Z3RO precoder.

### B. Multi-User Case

When multiple users are present, both the inter-user interference and distortion to multiple users have to be mitigated. In this more complex scenario, there is no closed-form solution available for the optimal precoder. As such, the NN is trained to learn how to perform this task. In Fig. 4, a comparison with the ZF precoder is made. In this figure, the cumulative distribution function (CDF) of the sum rate is depicted for 2000 channel realizations, when using the polynomial PA model from (4), for  $K \in \{2, 4, 6\}$ . When  $K = 2$  we see an increase in sum rate of 9.48 bit/channel use, when using the proposed method, 6.73 bit/channel use when  $K = 4$  and 3.05 bit/channel use if  $K = 6$ . This shows the ability of the NN to cancel non-linear distortion in the multi-user scenario, which results in significant increases in capacity. Additionally, this illustrates that the higher the number of users becomes, the less gain is to be obtained by using the NN precoder. This is to be expected as non-linear distortion is more spatially spread out when more users are present [20]. In other words, less distortion is beamformed in the user directions, which leads

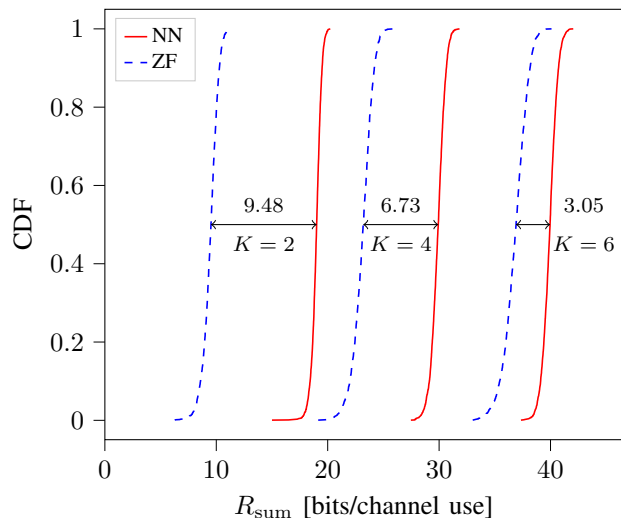


Fig. 4. CDF of the sum rate over 2000 channel realizations taken from the test set, for  $M = 64$ ,  $K \in \{2, 4, 6\}$  and  $P_T/\sigma_v^2 = 20$  dB. Comparing the NN precoder against ZF for the third-order PA model.

to less potential gains for mitigating this distortion. Moreover, when more users are present, canceling all distortion to all users becomes more complex. Hence, the solution found by the NN might not be the globally optimal one. Nevertheless, the NN-based precoder achieves a significant increase in channel capacity as compared to the classical ZF precoding.

In Fig. 5, the sum rate is depicted as a function of  $P_T/\sigma_v^2$  for  $K \in \{2, 4\}$ . It is shown that the proposed solution can outperform a perfect DPD (20) combined with ZF, when the system is highly distortion limited (i.e., for high signal-to-noise ratio (SNR) levels). This can be explained by the fact that a perfect DPD can only account for weakly non-linear effects, i.e., the PA can only be linearized up to the saturation point, after which clipping occurs.

Fig. 6 depicts the sum rate when  $p_{in}$  is fixed but  $p_{sat}$  is varied, resulting in a varied IBO. This shows that, for  $K \in \{2, 4\}$ , the NN always outperforms the classical ZF precoder, when evaluated using the polynomial PA model in (4). For instance, when  $K = 4$ , in order to achieve a sum rate of 30 bits/channel use, the ZF precoder requires  $-6$  dB back-off while the one generated by the NN only requires  $-3$  dB, implying a significant increase in energy efficiency. Additionally, when  $K = 2$ , the NN is able to achieve a nearly constant sum rate over a wide range of IBO. This illustrates the ability of the NN to suppress nearly all third-order distortion. When comparing the NN with ZF plus a perfect DPD in Fig 6, it is evident that the NN is most beneficial when a lot of distortion is present, i.e., at low back-off. However, we stress the fact that the NN does not have to be used as a replacement, but could be used in combination with DPD. When (perfect) DPD is available, the PA characteristic after applying DPD can be modeled as a polynomial on which the NN can be retrained. As such, the combination of both approaches could produce even better results.

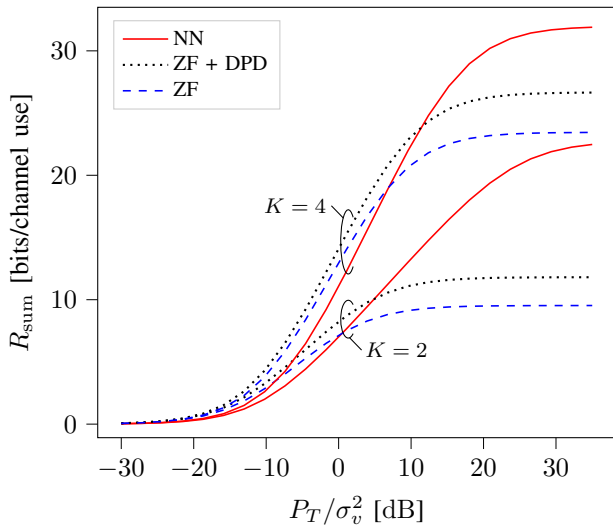


Fig. 5. Achievable rates averaged over 500 channel realizations taken from the test set, for  $M = 64$ ,  $K \in \{2, 4\}$  and  $\text{IBO} = -3$  dB. Comparing the NN precoder against ZF and ZF plus a perfect DPD (20).

## V. CONCLUSION

In this study, a CCNN is trained in a self-supervised manner to learn the mapping between channel matrix and linear precoding matrix in the presence of non-linear PA distortion. By learning this mapping, PAs can be operated closer to saturation implying a more energy-efficient operating point. Simulation results indicate that the proposed solution outperforms classical precoding schemes such as ZF. This conclusion holds even when ZF is combined with perfect DPD, given that the system is distortion-limited, i.e., in an energy-efficient regime. These results are especially promising in the multi-user case where no closed-form solutions for the precoder are available. Future perspectives include the use of GNNs which enable a lower complexity and allow for the incorporation of additional knowledge. For instance, currently, the system has to be retrained when the PA parameters or operating SNR changes. This could be avoided by incorporating the SNR and PA parameters as inputs to the network. Additionally, the third-order PA model is only valid when entering the saturation regime. Future work should adopt more complex PA models that capture higher-order and memory effects. Finally, the impact of channel estimation and PA parameter estimation errors on the performance of the proposed method has to be evaluated in future studies.

## REFERENCES

- [1] L. Belkhir and A. Elmeligi, "Assessing ICT global emissions footprint: Trends to 2040 & recommendations," *Journal of Cleaner Production*, vol. 177, pp. 448–463, Mar. 2018.
- [2] European Commission, "The European Green Deal," *COM (2019)*, November 2019.
- [3] United Nations, "The 2030 Agenda and the Sustainable Development Goals: An opportunity for Latin America and the Caribbean," (LC/G.2681-P/Rev.3), Santiago, 2018.
- [4] G. Auer, V. Giannini, C. Desset, I. Godor, P. Skillemark, M. Olsson, M. A. Imran, D. Sabella, M. J. Gonzalez, O. Blume, and A. Fehske, "How much energy is needed to run a wireless network?" *IEEE wireless communications*, vol. 18, no. 5, pp. 40–49, 2011.

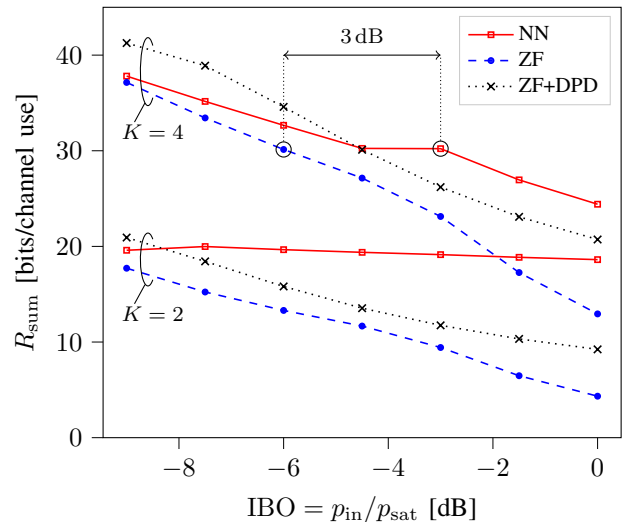


Fig. 6. Achievable sum rates averaged over 500 channel realizations of the test set.  $M = 64$ ,  $K \in \{2, 4\}$ ,  $P_T/\sigma_v^2 = 20$  dB with varied IBO. Comparing the NN, ZF and ZF plus DPD (20). The NN is retrained at each IBO point.

- [5] H. Bogucka and A. Conti, "Degrees of freedom for energy savings in practical adaptive wireless systems," *IEEE Communications Magazine*, vol. 49, no. 6, pp. 38–45, 2011.
- [6] S. Cripps, *RF Power Amplifiers for Wireless Communications*, ser. Artech House Microwave Library. Norwood: Artech House, 2006.
- [7] F. Rottenberg, G. Callebaut, and L. Van der Perre, "Z3RO Precoder Cancelling Nonlinear Power Amplifier Distortion in Large Array Systems," in *ICC 2022 - IEEE International Conference on Communications, 2022*, pp. 432–437.
- [8] —, "The Z3RO Family of Precoders Cancelling Nonlinear Power Amplification Distortion in Large Array Systems," *IEEE Transactions on Wireless Communications*, pp. 1–1, 2022.
- [9] T. Feys, G. Callebaut, L. Van der Perre, and F. Rottenberg, "Measurement-Based Validation of Z3RO Precoder to Prevent Nonlinear Amplifier Distortion in Massive MIMO Systems," in *2022 IEEE 95th Vehicular Technology Conference: (VTC2022-Spring)*, 2022, pp. 1–5.
- [10] S. R. Aghdam, S. Jacobsson, U. Gustavsson, G. Durisi, C. Studer, and T. Eriksson, "Distortion-Aware Linear Precoding for Massive MIMO Downlink Systems with Nonlinear Power Amplifiers," 2020. [Online]. Available: <https://arxiv.org/abs/2012.13337>
- [11] T. Schenk, *RF Imperfections in High-rate Wireless Systems: Impact and Digital Compensation*, 1st ed. Dordrecht: Springer Netherlands, 2008.
- [12] O. T. Demir and E. Bjornson, "The Bussgang Decomposition of Non-linear Systems: Basic Theory and MIMO Extensions [Lecture Notes]," *IEEE Signal Processing Magazine*, vol. 38, no. 1, pp. 131–136, 2021.
- [13] P. W. Battaglia *et al.*, "Relational inductive biases, deep learning, and graph networks," 2018. [Online]. Available: <https://arxiv.org/abs/1806.01261>
- [14] B. Zhao, J. Guo, and C. Yang, "Learning Precoding Policy: CNN or GNN?" in *2022 IEEE Wireless Communications and Networking Conference (WCNC), 2022*, pp. 1027–1032.
- [15] G. Philipp, D. Song, and J. G. Carbonell, "Gradients explode - deep networks are shallow - resnet explained," 2018. [Online]. Available: <https://openreview.net/forum?id=HkpYwMZRb>
- [16] A. Araujo, W. Norris, and J. Sim, "Computing receptive fields of convolutional neural networks," *Distill*, 2019, <https://distill.pub/2019/computing-receptive-fields>.
- [17] D. P. Kingma and J. Ba, "Adam: A method for stochastic optimization," 2014. [Online]. Available: <https://arxiv.org/abs/1412.6980>
- [18] C.-S. Choi *et al.*, "RF impairment models for 60GHz-band SYS/PHY simulation," *Project: IEEE P802.15 Working Group for Wireless Personal Area Networks (WPANs)*, p. 17, 2006.
- [19] Nokia, "Realistic power amplifier model for the New Radio evaluation," *3GPP TSG-RAN WG4 Meeting 79, R4-163314*, May 2016.
- [20] C. Mollen, U. Gustavsson, T. Eriksson, and E. G. Larsson, "Spatial Characteristics of Distortion Radiated From Antenna Arrays With Transceiver Nonlinearities," *IEEE transactions on wireless communications*, vol. 17, no. 10, pp. 6663–6679, 2018.